Concentration Dependence of IgG-Protein A Affinity Studied by Wireless-Electrodeless QCM

Hirotsugu Ogi, Kazuma Motohisa, Kenichi Hatanaka,

Toshinobu Ohmori, Masahiko Hirao

Graduate School of Engineering Science, Osaka University

Machikaneyama 1-3, Toyonaka, Osaka 560-8531, Japan

Masayoshi Nishiyama

Central Workshop, Osaka University

Machikaneyama 1-3, Toyonaka, Osaka 560-8531, Japan

Abstract

The binding affinity between human immunoglobulin G (IgG) and protein A was studied by the homebuilt wireless-electrodeless quartz crystal microbalance (QCM). Protein A was immobilized on the electrodeless AT-cut quartz plate of 0.05 mm thick and its fundamental resonance frequency near 34 MHz was measured by a noncontacting manner using a line antenna. The vibrational analysis was performed to ensure higher sensitivity of the electrodeless QCM. A flow-cell system was fabricated to continuously measure the resonance frequency during the injection sequence of the IgG solutions with concentrations of 1-20,000 ng/mL. The exponential frequency changes were recorded to determine the affinity based on the Langmuir kinetics. The equilibrium constant K_A significantly varied between 6×10^6 and 6×10^{10} M^{-1},

depending on the IgG concentration, which is attributed to various formations of IgG-protein A complexes.

Key words: affinity, electrodeless, QCM, IgG, protein A, wireless

1 Introduction

Quartz crystal microbalance (QCM) has shown pronounced ability for studying recognition behavior among biochemical molecules through changes of resonance frequencies of the quartz plate. The surface-modified quartz plate adsorbs target molecules, resulting in the increase of the effective mass of the resonator system and then in the decrease of the mechanical resonance frequencies (Sauerbrey (1959)). The resonance frequency can be monitored during the binding reactions in real time without any labeling, yielding thermodynamic binding constants (Eddowes (1987); Liu *et al.* (2003a,b)). It has been therefore a powerful tool for studying interactions among various biomolecules (Muramatsu *et al.* (1987); Pan & Shih (2004); Liu *et al.* (2003a,b); Suri *et al.* (1994); Zhou *et al.* (2004); Caruso *et al.* (1997); Larsson *et al.* (2003); Su *et al.* (2004); Stengel *et al.* (2005); Halámek *et al.* (2002)).

Significant breakthrough in the QCM measurement must be an electrodeless technique, because it avoids deterioration of the sensitivity caused by the metallic electrodes deposited on both surfaces: The use of a thinner quartz plate achieves higher sensitivity, but unfavorable effect of the electrode layers to the sensitivity becomes more significant as well (Ogi *et al.* (2006a)). Therefore, the electrodeless technique is the desired answer for achieving a high-sensitive QCM. Another advantage of the electrodeless approach is that it allows the use of various coating materials on the oscillator, even a non-

conductive CVD diamond film, which shows high affinity to human body and extremely high stability.

Recently, a few researchers presented electrodeless biosensors. Thompson *et al.* (2003) used an rf spiral coil located beneath an electrodeless quartz crystal and detected resonance frequencies. Vasilescu *et al.* (2005) used the same technique for $GaPO_4$ as a candidate biosensor. Their methods using spiral coils, however, allowed a very small air gap ($\sim$30 μm) between coils and piezoelectric plates, making the isolation of the crystal unrealistic. Ogi *et al.* (2006b) developed an isolated electrodeless nickel oscillator using a meander-line coil through the piezomagnetic effect. Ogi *et al.* (2006a) then developed a wireless-electrodeless QCM using the line antenna and completely isolated it from the antenna: It showed higher sensitivity in the detection of human immunoglobulin G (IgG).

In the present study, we study the affinity between IgG and staphylococcal protein A (SPA). Although their high affinity has been recognized by many researchers, the dependence of the affinity on their concentrations was not quantitatively studied by QCM because of the lower sensitivity of the conventional QCM; most of the previous studies used QCMs with the fundamental resonance frequencies smaller than 10 MHz. Here, we use a thinner electrodeless QCM (0.05 mm) to investigate the dependence of their affinity on the IgG concentration. Protein A binds the Fc portion of certain types of IgG (Kronvall*et al.* (1970a); Kessler (1975); O'Keefe and Bennett (1980)). Their binding affinity is affected by their molar relation, and the reported values by several researchers alter each other. We then investigate the affinity for a wider concentration range of IgG between 1 ng/mL and 20 μg/mL to demonstrate the sensitivity and usefulness of the wireless-electrodeless QCM.

2 Electrodeless QCM

Figure 1(a) shows the homebuilt electrodeless QCM cell. The 0.05-mm thick AT-cut quartz plate with 5×4 mm^2 area is sandwiched by the silicon-rubber sheets and placed inside the cell. The volume capacity of the cell is 0.27 mL. The line antenna is embedded in the bottom wall made of the acrylate resin. The distance between the antenna and the quartz crystal is 1.5 mm, achieving the noncontacting measurement. The antenna consists of three straight wires; two for generation and detection of the through-thickness resonance vibration, and the other for grounding.

We applied the tone-burst voltage to the generation wire to radiate the quasistatic electric field, which caused the pure shear plane wave propagating in the thickness direction through the converse piezoelectric effect. After the excitation, the detection wire detected the mechanical vibrations of the crystal through the piezoelectric effect. The received signals entered the superheterodyne spectrometer, and the amplitude and phase at the same frequency component as the driving signal were recorded (Hirao and Ogi (2003)). A frequency scan yielded the resonance spectrum and the Lorentzian-function fitting provided the resonance frequency (the frequency-scan method). Because this frequency-scan mode required relatively longer time, we monitored the phase of the received signal at the fixed frequency after the resonance frequency became sufficiently stable to determine the resonance-frequency change from the linear relationship between the phase and frequency near the resonance frequency (the phase method).

The surface of the oscillator was modified by the gold-thiol modification. A

9-nm thick Au film was deposited after 1-nm thick Cr film on one side of the crystal. This Au film was used for making the gold-thiol binding effective, not for an electrode. (A 9-nm thick electrode little affects the QCM sensitivity as seen later in Fig. 5.) The crystal was cleaned in the piranha solution (98%H_2SO_4:33%H_2O_2=4:1). After rinsing with ultrapure water, it was immersed in 50 μM 5-carboxy-1-pentanethiol/ethanol solution for 3 h. The surface was activated by 100 mM EDC (1-ethyl-3-(3-dimethylaminopropyl)carbodiimide, hydrochloride) solution and 100 mM sulfo-NHS (N-hydroxysulfosuccinimide sodium salt) solution. Protein A was then immobilized on the surface by immersing the oscillator into the phosphate-buffer solution (PBS, pH 7.0) containing 1 mg/ml protein A for 24 h at 4 °C. The remaining activated ester sites were blocked with a 0.1 M glycine solution.

Human IgG was from Athens Research and Technology, Inc. (product num. 16-16-090707; purity ∼95%). Protein A was from Zymed Laboratories, Inc. (product num. 10-1100; purity 98%). 5-carboxy-1-pentanethiol (product num. C387) and EDC (product num. W001) were from Dojindo Laboratories. Sulfo-NHS was from Sigma-Aldrich Japan (product num. 56485). All of other chemical substances were purchased from Wako Pure Chemical Industries Ltd.

The QCM cell is installed into the homebuilt flow-cell system shown in Fig. 1(b). The temperature inside the cell was kept at 37± 0.02 ° C. PBS steadily flows as the carrier fluid with a flow rate of 0.18 ml/min. We first monitored the fundamental resonance frequency near 34 MHz by the frequency-scan method, which took about 10 s for one measurement. After the resonance frequency became stable (frequency fluctuation $< 10^{-7}$), we switched the measurement mode to the phase method to make a quicker measurement (∼0.1 s). The IgG solution (PBS containing small amount of IgG) was then injected, which was

followed by the injection of glycine-HCl buffer (0.1 M, pH 2.2) for dissociating IgG molecules from protein A, and by the injection of the carrier PBS. This injection sequence (PBS, IgG, glycine-HCl, PBS, $\cdots$) was repeated with various IgG concentrations.

3 RESULTS

Figure 2 shows the typical response of the resonance frequency during the injection sequence. Injections of the IgG solutions decreased the resonance frequency and the amount of the frequency change increased with the increase of the IgG concentration as shown in Fig. 3 (the error bar indicates the coefficient of variation of the frequency fluctuation.) The frequency change obeyed the exponential-decay law as shown in Fig. 4. We note that the spikes in the frequency change were caused by the injection of the glycine-HCl solution (Fig. 2), which is unusual in a conventional QCM measurement. The principal reason will be the difference of the dielectric constant of the glycine HCl solution, because the naked crystal surface allows the electrical coupling between the crystal and the surrounding fluid (Rodahl *et al.* (1996)). In other words, this QCM can be a dielectric sensor. However, because we used the frequency response in the same surrounding liquids (IgG solutions) in the analysis, this effect cannot be included.

4 DISCUSSIONS

The fractional frequency change caused by adsorption of the target molecules is estimated by (Sauerbrey (1959))

$$\frac{\Delta f}{f} = -\frac{\Delta m}{M_q} \tag{1}$$

Here, M_q and Δm denotes the mass of the quartz crystal and that of the adsorbed molecules, respectively. Viscosity and mass of surrounding liquid also contribute to the decrease of the resonance frequency and their influence has been estimated through the square-root dependence of the frequency (Kanazawa and Gordon (1985); Martin *et al.* (1991))

$$\frac{\Delta f}{f} = -\frac{1}{\sqrt{f}} \frac{A_q}{M_q} \sqrt{\frac{\rho_l \eta_l}{4\pi}} \tag{2}$$

Here, A_q is the effective area of the crystal, and ρ_l and η_l are the mass density and the shear viscosity of the surrounding liquid. Thus, the higher frequency we use, the less significant the frequency change caused by the viscosity effect becomes, compared with the mass-loading effect. Therefore, a high-frequency (or thinner) QCM is required to avoid the overestimation of the adsorbed mass and to analyze the kinetics of the binding reaction quantitatively. The sensitivity of a thinner QCM is, however, deteriorated by the electrodes deposited on both surfaces as indicated in our previous study (Ogi *et al.* (2006a)). We therefore investigate the effect of the electrodes on the frequency sensitivity for the present QCM to demonstrate the advantage of the electrodeless approach.

The through-thickness resonance frequencies in a multilayered plate can be analytically calculated when thicknesses, mass densities, and moduli of indi-

vidual layers are given (Ogi *et al.* (2002)). We calculated the fractional amount of the frequency decrease when the IgG layer is densely adsorbed on the electrodes by changing the total thickness of the electrodes. The thickness of the quartz plate was fixed to 50 μm. The thickness and mass density of the IgG layer were assumed as 10 nm and 1,500 kg/m^3, referring to the reported IgG structure (Sarma *et al.* (1971); Nollb *et al.* (1982)). (Although the thickness would be determined experimentally using AFM for example, our purpose is to show the disagreement of the conventional Sauerbrey equation when the electrodes are deposited. Considering the ambiguity of the shear modulus of the IgG layer, which affects also the frequency change, this roughly estimated thickness is acceptable for this purpose.)

A representative result for gold electrodes is shown in Fig. 5. This result indicates three important facts. Fist, the frequency sensitivity is deteriorated as the electrode thickness increases. A 300 nm thick electrodes on both sides, for example, degenerate the sensitivity by 15 % at least. Second, the Sauerbrey equation fails to predict the frequency change when the electrodes are deposited. Third, the sensitivity is affected by the shear modulus of the adsorbed layer (the elastic coupling effect (Ogi *et al.* (2006a)). We deposited the 9-nm thick Au layer on one side of the crystal for making the organic monolayer, but the result in Fig. 5 shows that it hardly influences the frequency sensitivity and that the Sauerbrey equation applies with a negligible error.

Next, the binding affinity is analyzed from the frequency response. Binding reactions between two biomolecules are characterized by three kinetic constants; the association rate constant k_a, the dissociation rate constant k_d, and the equilibrium constant $K_A = k_a/k_d$, which quantities thermodynamic behavior at the equilibrium condition and represents the binding affinity. The

relationship between the frequency change and the kinetics of the binding reaction are given by (Eddowes (1987); Liu *et al.* (2003a,b))

$$\frac{\Delta f(t)}{f_0} = A\left\{\mathrm{e}^{-(k_a C_{\mathrm{IgG}} + k_d)t} - 1\right\} \tag{3}$$

$$\frac{1}{\Delta f_e} = \frac{1}{\Delta f_{max}} + \frac{1}{\Delta f_{max} K_A} \cdot \frac{1}{C_{\mathrm{IgG}}} \tag{4}$$

Where $\Delta f(t) = f_0 - f(t)$ is the frequency decrement caused by the binding reaction, and f_0 is the frequency before the reaction. Δf_e is the frequency change at the equilibrium state, and Δf_{max} denotes the possible maximum frequency change which would occur when all the immobilized protein-A molecules were bound with IgG. C_{IgG} represents the IgG concentration in the QCM cell. A is a constant. Thus, the plot C_{IgG}^{-1} versus Δf_e^{-1} yields a straight line, providing the affinity K_A through its slope and intercept. Equation (3) indicates that the frequency decrease obeys an exponential function, which is supported by the observation in Fig. 4.

As shown by the broken line in Fig. 6, the relationship between C_{IgG}^{-1} and Δf_e^{-1} cannot be explained by a single line, but by multiple lines, indicating that the binding affinity depends on the concentration of IgG. Table 1 shows K_A values determined for three IgG concentration regions. (Each affinity value was derived from three measurement points.) The equilibrium constant drastically increases with the decrease of the IgG concentration.

IgG-Fc regions possess two functional protein A binding sites near the outer interfaces between C_H2 and C_H3 domains, and protein A contains four monovalent Fc-binding sites (Deisenhofer (1981)). The molar ratio of IgG to protein A to construct a complex is close to one in larger protein A excess, whereas it asymptotically approaches to two in larger IgG excess (Hanson and Shumaker

(1984)). Both of two binding sites of IgG can interact with protein A with a larger ratio of protein A molecules to IgG molecules, achieving a high affinity. However, the number of the monovalent IgG-protein A binding will increase with a larger IgG molecules, decreasing the affinity, because of the hindrance effect.

Several previous researches support the observed concentration dependence of the IgG-SPA binding affinity: Early study by Kronvall *et al.* (1970b) provided the affinity 4.5×10^7 M^{-1} for the binding between IgG and intact SPA on the bacterium. The affinity between the monovalent fragment FB of SPA and the intact rabbit IgG was studied by the fluorescence titration method, which yielded the affinity 3×10^6 M^{-1} (Lancet *et al.* (1978)). These previous results indicate higher affinity for the binding with polyvalent reactants. Kessler (1975) indicated two affinity regions with respect to the SPA concentration, and yielded K_A=2.0×10^8 M^{-1} and 2.0×10^6 M^{-1} for higher and lower concentrations of SPA, respectively. O'Keefe and Bennett (1980) supported the enhanced affinity at lower IgG concentrations and for longer incubations with radioimmunoassay. Therefore, our values are compared with the results by previous studies without significant contradiction, although the K_A value would be affected by liquid conditions such as pH, temperatures, and ionic strength and so on, and the conditions used in the individual researches were not the same.

The concentration dependence of the affinity of IgG-protein A observed here is attributed to the different structure of the IgG-protein A complex. Hanson and Shumaker (1984) suggested five plausible structures for IgG-protein A complexes, depending on their molar ratio. Individual complex structures may possess different affinity.

5 CONCLUSION

The homebuilt wireless-electrodeless high-frequency QCM was developed for studying the affinity among biomolecules. The fundamental shear vibration of the 50 μm thick AT-cut quartz crystal plate was excited and detected by the line antenna with the noncontacting manner without using electrodes. The vibrational analysis showed higher sensitivity of an electrodeless QCM. The homebuilt QCM method was used to study the binding affinity between IgG and protein A in the IgG concentration range between 1 and 20,000 ng/mL. The affinity varied highly depending on the IgG concentration between 6×10^{6} M^{-1} and 6×10^{10} M^{-1}; lower concentration provided higher affinity. Thus, the wireless-electrodeless high sensitive QCM technique contributes to the study of binding affinity among various biomolecules. Currently, the detection limit and dynamic range are $\sim$500 pg/ml and 500 pg/ml-0.1 mg/ml, respectively. These values will be improved more by using thinner electrodeless QCMs in near future.

References

Caruso, F., Rodda, E., Furlong, DN., Niikura, K., & Okahata, Y., 1997. Anal. Chem. 69, 2043-2049.

Deisenhofer, J., 1981. Biochem. 20, 2361-2370.

Eddowes, M. J., 1987. Biosensors. 3, 1-15.

Halámek, J., Makower, A., Skládal, P. & Scheller, F., 2002. Biosensors & Bioelectronics. 17, 1045-1050.

Hanson, DC. & Schumaker, VN., 1984. J. Immunol. 132, 1397-1409.

Hirao, M. & Ogi, H., 2003. EMATs for Science and Industry: Noncontacting Ultrasound Measurements (Springer-Kluwer, Boston).

Kanazawa, K.K., & Gordon, J.G., 1985. Anal. Chim. Acta. 175, 99-105.

Kessler, S. W., 1975. J. Immunol. 115, 1617-1624.

Kronvall, G., Seal, U. S., Finstad, J. Williams, R. C. Jr., 1970a. J. Immunol. 104, 140-147.

Kronvall, G., Quie, P. G., Williams, R. C. Jr., 1970b. J. Immunol. 104, 273-278.

Lancet, D., Isenman, D., Sjödahl, J., Sjöquist, J., & Pecht, I., 1978. Biochem. Biophys. Res. Commun., 85, 608-614.

Larsson, C., Rodahl, M., & Hook, F., 2003. Anal. Chem. 75, 5080-5087.

Liu, Y., Yu, X., Zhao, R., Shangguan, D., Bo, Z. & Liu, G., 2003a. Biosensors & Bioelectronics. 18, 1419-14279.

Liu, Y., Yu, X., Zhao, R., Shangguan, D., Bo, Z. & Liu, G., 2003b. Biosensors & Bioelectronics. 19, 9-19.

Martin, S. J., Granstaff, V. E., & Frye, G. C., 1991. Anal. Chem. 63, 2272-2281.

Muramatsu, H., Dicks, M. D., Tamiya, E. & Karube, I., 1987. Anal. Chem.. 59, 2760-2763.

Nollb, F, Lutscha, G & Bielkab, H., 1982. Immunology Lett. 4, 117-123.

O'Keefe, E. & Bennett, V., 1980. J. Biol. Chem. 25, 561-568.

Ogi, H., Shimoike, G., Hirao, M., Takashima, K., & Higo, Y., 2002. J. Appl. Phys. 91, 4857-4862.

Ogi, H., Motohisa, K., Matsumoto, T., Hatanaka, K. & Hirao, M., 2006a. Anal Chem. 78, 6903-6909.

Ogi, H., Motohisa, K., Matsumoto, T., Mizugaki, T., & Hirao, M., 2006b. Biosens. & Bioelectron. 21, 2001-2005.

Pan, N. Y. & Shih, J. S., 2004. Sensors & Actuators B. 98, 180-187.

Rodahl, M., Hook, F., & Kasemo, B., 1996. Anal. Chem. 68, 2219-2227.

Sarma, V., Silverton, E., Davies, D. & Terry, W., 1971. J. Biol. Chem. 246, 3753-3759.

Sauerbrey, G., 1959. Z. Phys. 155, 206-222.

Stengel, G., Höök, F., & Knoll, W., 2005. Anal. Chem. 77, 3709-3714.

Su, X., Robelek, R., Wu, Y., Wang, G., & Knoll, W., 2004. Anal. Chem. 76, 489-494.

Suri, C. R., Raje, M. & Mishra, G. C., 1994. Biosensors & Bioelectronics. 9, 535-542.

Thompson, M., Ballantyne, S., Cheran, L., Stevenson A., & Lowe C., 2003. Analyst. 128, 1048-1055.

Vasilescu, A., Ballantyne, S., Cheran L., & Thompson M., 2005. Analyst. 130, 213-220.

Zhou, C., Friedt, J., Angelova, A., Choi, K., Laureyn, W., Frederix, F., Francis, A., Campitelli, A., Engelborghs, Y., & Borghs, G., 2004. Langmuir. 20, 5857-5878.

Tables

Table 1

Dependence of the equilibrium constant K_A on the IgG concentration, C_{IgG}.

C_{IgG} (μg/mL)	5-20	0.1-5	0.001-0.1
K_A (M^{-1})	6.2×10^{6}	9.0×10^{8}	6.0×10^{10}

Figure Caption

Fig. 1 (a)The homebuilt isolated-electrodeless QCM. The 50-μm thick AT-cut quartz plate is located inside the cell, and it is fixed by the silicon rubber sheets. The line antenna, consisting of generation, detection, and grounding wires measures the resonance frequency contactlessly. (b)The homebuilt QCM flow cell system. All measurements have been done at a constant temperature of 37 ° C

Fig. 2 An example of the frequency response by the injection sequence. Arrows indicate arrival times of the solutions injected.

Fig. 3 Relationship between the IgG concentration and the amount of the frequency decrease.

Fig. 4 Behavior of the frequency change caused by the injections of the IgG solutions. The inlet shows the binding curve for the injection of the lowest concentration IgG solution of 1 ng/mL(=6.7×10^{-12}M)

Fig. 5 Effect of the frequency sensitivity on the total thickness of the gold electrode calculated assuming three shear-modulus values of the adsorbed IgG layer, 0.1, 1, and 10 MPa.

Fig. 6 Relationship between C_{IgG}^{-1} and Δf_e^{-1}. The measurement cannot be explained by a single equilibrium constant (broken line). Three equilibrium constants are, then, used to fit equation (4) to the measurements (solid lines). Three data points were used for obtaining each affinity constant.

Note that the fitted lines curve because the logarithmic scales are used.

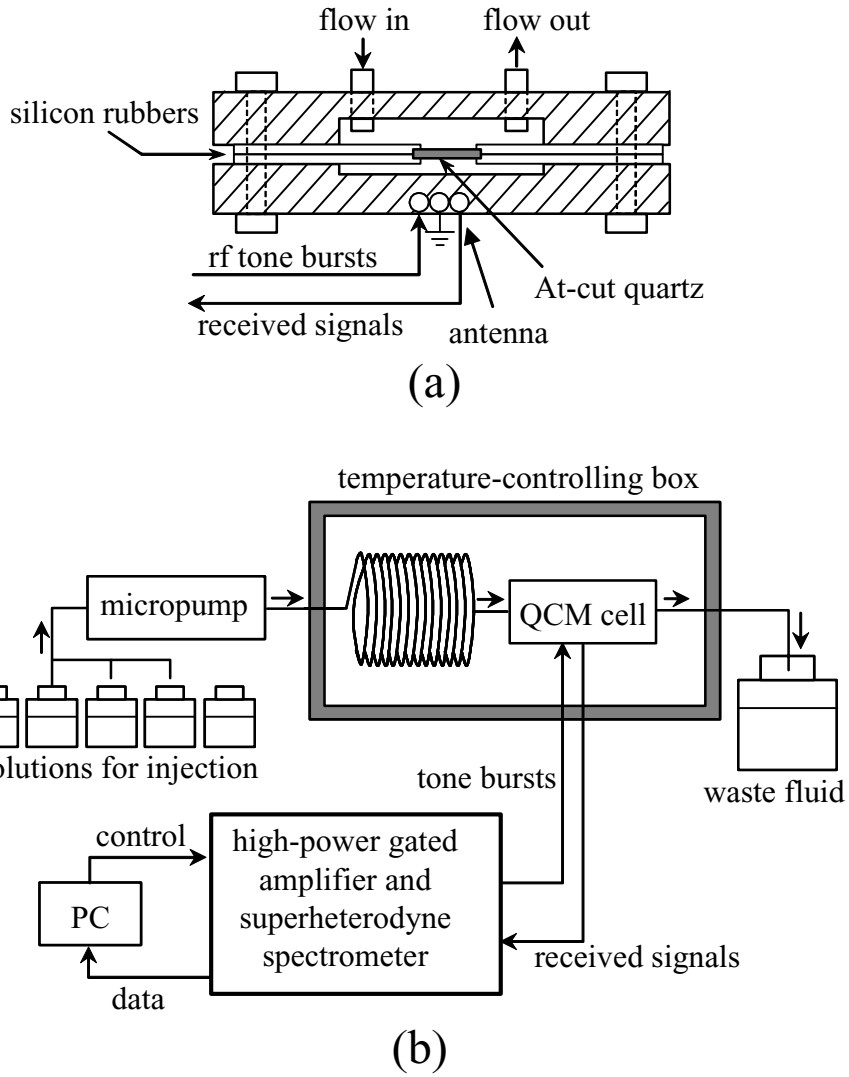
flow in
flow out
silicon rubbers
rf tone bursts
received signals
antenna
At-cut quartz
(a)
temperature-controlling box
micropump
QCM cell
solutions for injection
tone bursts
waste fluid
control
high-power gated
amplifier and
superheterodyne
spectrometer
PC
data
received signals
(b)

Fig. 1.

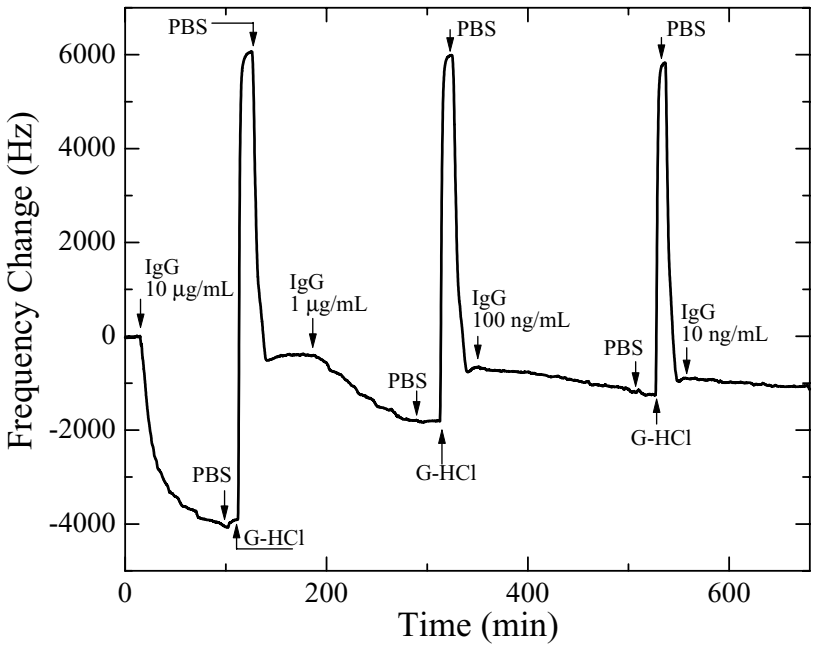
PBS
PBS
PBS
IgG
10 µg/mL
IgG
1 µg/mL
IgG
100 ng/mL
IgG
10 ng/mL
PBS
PBS
PBS
G-HCl
G-HCl
G-HCl
Frequency Change (Hz)
6000
4000
2000
0
-2000
-4000
0
200
400
600
Time (min)

Fig. 2.

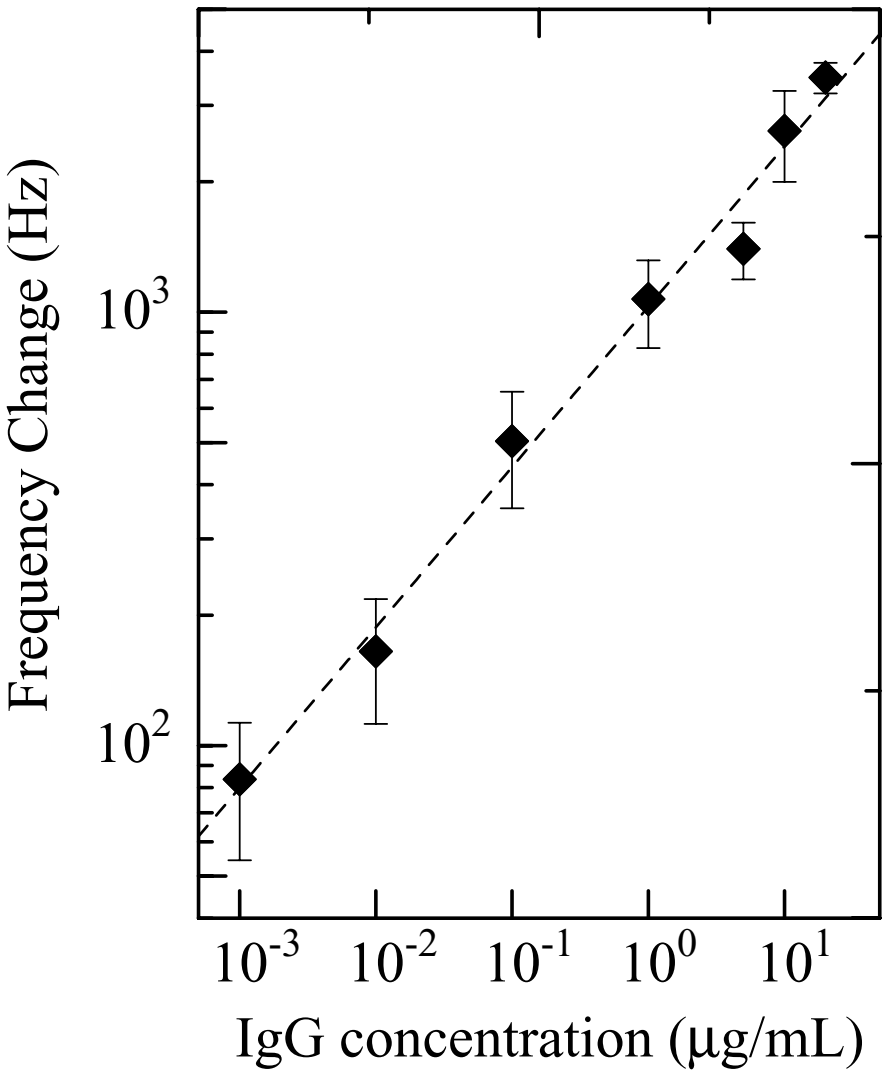
Frequency Change (Hz)
10^3
10^2
10^-3
10^-2
10^-1
10^0
10^1
IgG concentration (μg/mL)

Fig. 3.

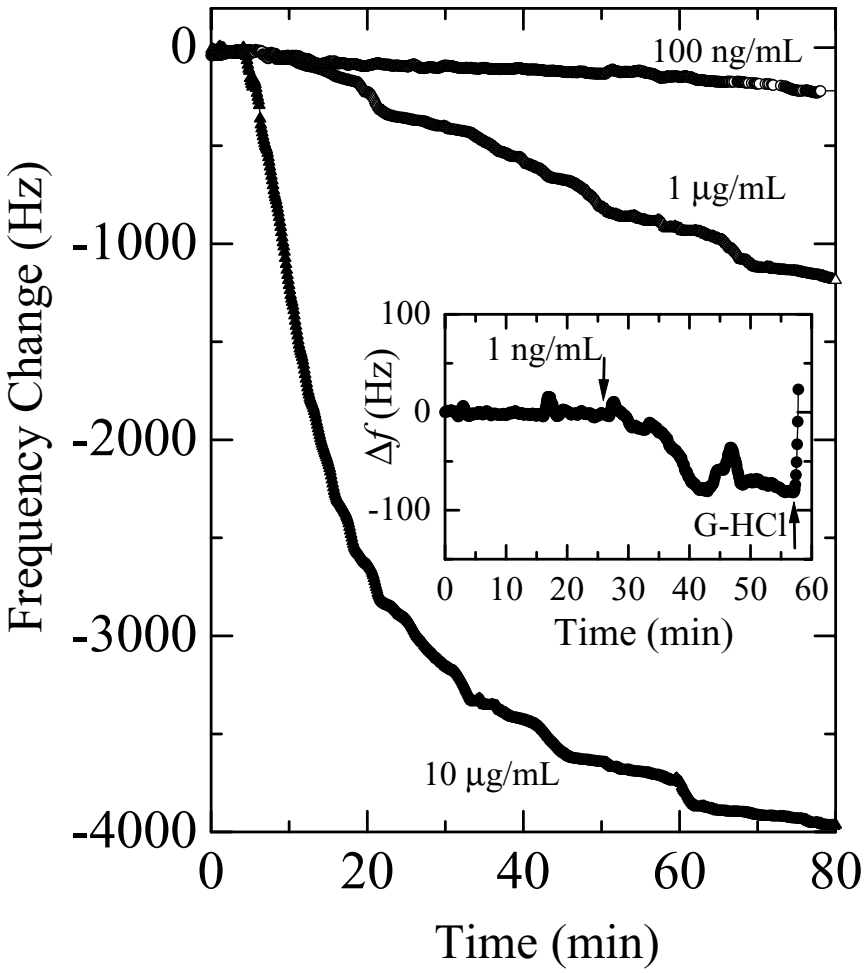
0
-1000
-2000
-3000
-4000
Frequency Change (Hz)
0
20
40
60
80
Time (min)
100 ng/mL
1 μg/mL
10 μg/mL
100
0
-100
Δf (Hz)
1 ng/mL
G-HCl
0
10
20
30
40
50
60
Time (min)

Fig. 4.

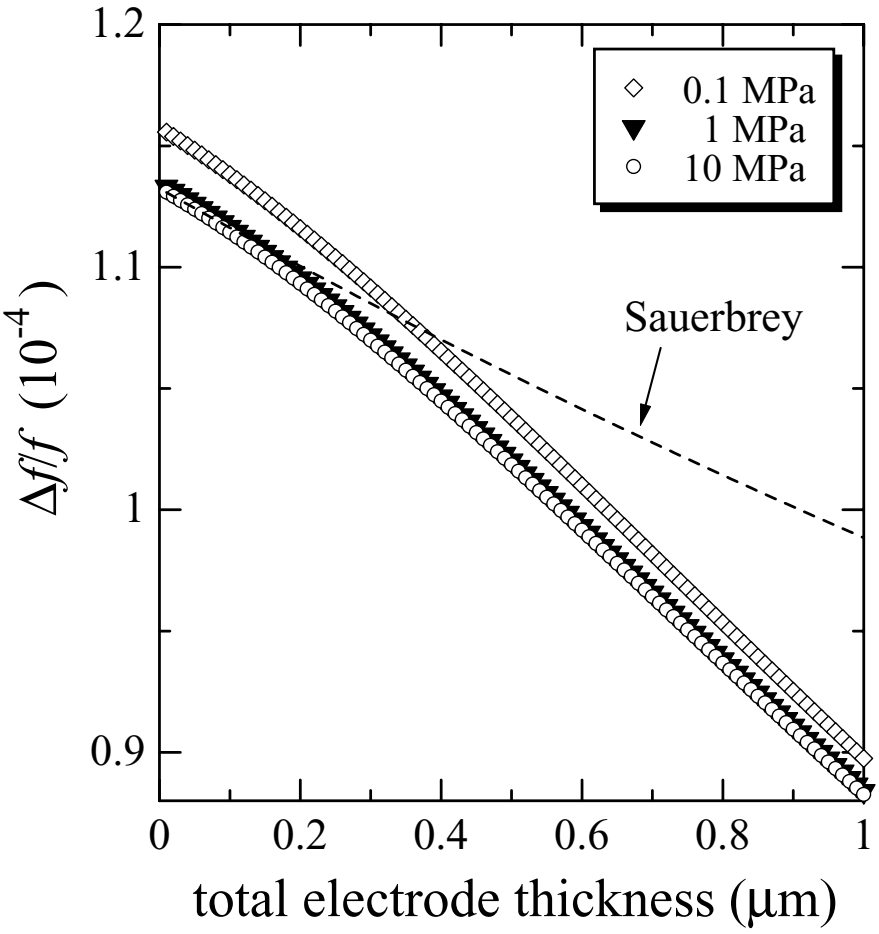
1.2
1.1
1
0.9
0
0.2
0.4
0.6
0.8
1
0.1 MPa
1 MPa
10 MPa
Sauerbrey
Δf/f (10^-4)
total electrode thickness (μm)

Fig. 5.

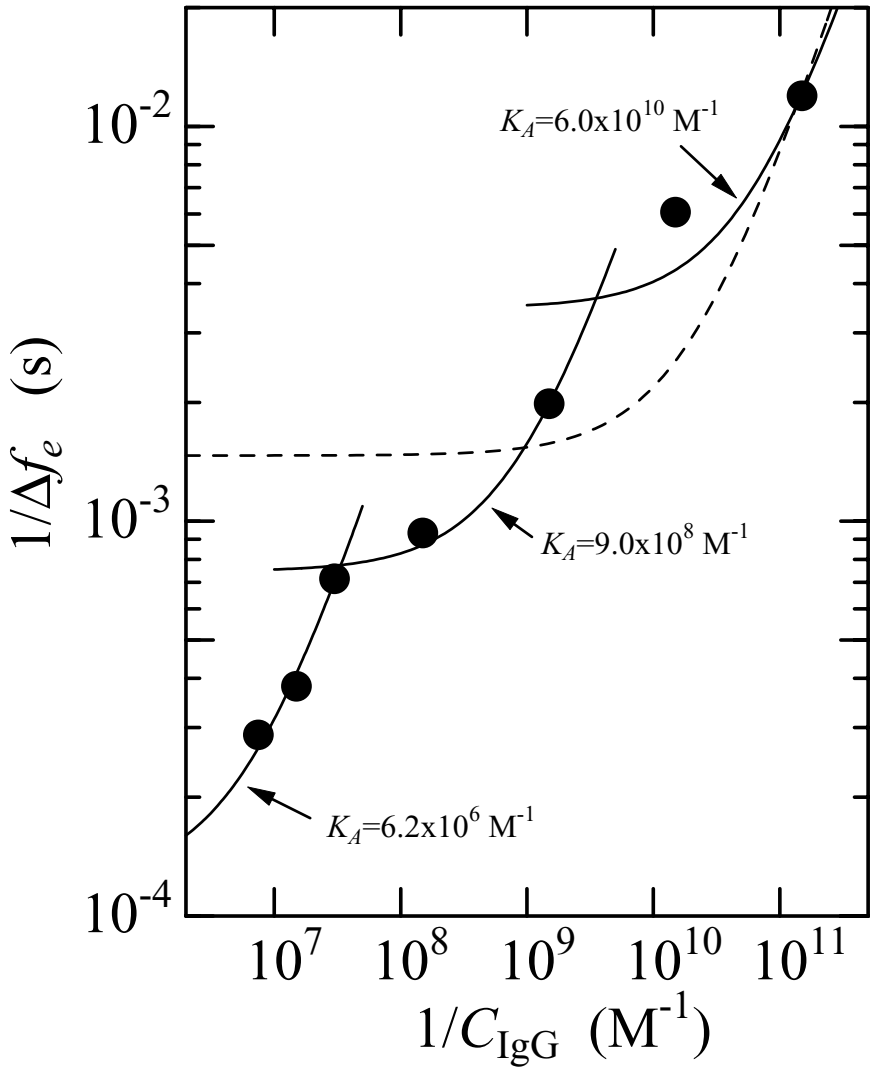
10^{-2}
10^{-3}
10^{-4}
$1/\Delta f_e$ (s)
K_A=6.0x10^{10} M^{-1}
K_A=9.0x10^{8} M^{-1}
K_A=6.2x10^{6} M^{-1}
10^{7} 10^{8} 10^{9} 10^{10} 10^{11}
$1/C_{\mathrm{IgG}}$ (M^{-1})

Fig. 6.